

Analysis of the $WW\gamma$ vertex: Form-factor and anomalous-magnetic-moment effects

J. A. Robinson and T. G. Rizzo

Ames Laboratory, Iowa State University, Ames, Iowa 50011

(Received 6 June 1985; revised manuscript received 13 January 1986)

We examine the possibility of placing limits on the composite structure of the W boson by looking for form-factor effects as well as a W anomalous magnetic moment (μ_W) in the processes $W \rightarrow e\nu\gamma$, $\gamma e \rightarrow W\nu$, and $\bar{\nu}e \rightarrow W\gamma$. We find the most sensitive reaction to variation in the magnetic-moment parameter κ_W is $\gamma e \rightarrow W\nu$, which should be accessible at the Stanford Linear Collider and CERN LEP. We find that all three processes are quite sensitive to form-factor effects for a compositeness scale in the range $100 < \Lambda < 350$ GeV. From these reactions future experiments should be able to observe W compositeness from the effects of a nonstandard κ_W , form factors, or both. If such effects are not observed, stringent limits on W compositeness can be obtained from these reactions.

I. INTRODUCTION

The discovery¹ of the W and Z bosons at CERN gives strong experimental confirmation of the standard electroweak model.² However, it is quite possible that the standard model (SM) is not a fundamental theory but simply a low-energy effective theory. Therefore, to determine if the observed W or Z is a fundamental gauge particle, rather than a composite object, a detailed study of its interactions must be carried out. If the W or Z is composite, we might expect (as in the case of hadrons composed of quarks) that the first indication of compositeness will be form-factor corrections to the propagator and/or couplings of the gauge bosons. Also, a composite W would very likely have an anomalous-magnetic-moment parameter (κ_W) which is significantly different from the gauge-theory value (apart from radiative corrections) of unity.

First we will consider form-factor corrections to the W propagator and to the gauge-boson trilinear ($WW\gamma$) coupling. To modify the W propagator we will multiply it by a function $F_p(q^2, \Lambda)$, which depends on the momentum transfer (q^2) of the virtual W and on the composite scale (Λ). It was argued in an earlier work³ that the simplest form for $F_p(q^2, \Lambda)$ is the function

$$F(q^2, \Lambda) = (1 + \lambda q^2 / \Lambda^2)^{-1}, \quad (1)$$

where $\lambda = \pm 1$ so that $\lambda q^2 > 0$. We see that as $\Lambda^2 \rightarrow \infty$ that $F \rightarrow 1$ and we obtain the SM. As mentioned above we also consider a correction to the trilinear coupling of the gauge bosons. We assume, as for the propagator case, that the vertex correction F_V is obtained by simply multiplying the SM coupling by the function given in (1). In our calculations we will consider all possible modifications to the cross section/decay rate: $F_p = 1, F_V \neq 1$; $F_p \neq 1, F_V = 1$; $F_p \neq 1, F_V \neq 1$. Although in any realistic theory the true modifications due to compositeness may be more complex we treat this simple case here to get a feeling for the magnitude of such effects.

For current low-energy experimental data if the composite scale is in the range $0.1 < \Lambda < 0.5$ TeV (the range which we will study in this paper), the form-factor contri-

bution would be negligible.⁴ However, as we will see, for q^2 of order Λ^2 , decay rates and cross sections may deviate substantially from their SM predictions. In the near future, accelerators will have center-of-mass energies which may be comparable to Λ , so that form-factor effects might become observable.⁵

Each of the interactions considered in this paper involves the coupling of a W boson to a photon. We find that deviations in the trilinear gauge-boson coupling ($WW\gamma$) produces cross section/decay rates which differ substantially from the SM results. In general a charged spin-one boson would have an anomalous magnetic (μ_W) and electric quadrupole moment (Q_W) given by⁶

$$\mu_W = \frac{e}{2M}(1 + \kappa_W + \lambda_W), \quad Q_W = -\frac{e}{M^2}(\kappa_W - \lambda_W),$$

where κ_W is the magnetic-moment parameter and λ_W is the quadrupole-moment parameter. The general $WW\gamma$ coupling including κ_W and λ_W has been determined⁶ and is quite complicated. Since our main purpose in this paper is to obtain the magnitude of composite-boson effects (therefore determining in which interactions compositeness effects may first be seen) we will make the simplifying assumption that λ_W is given by its SM value ($\lambda_W = 0$). This also reduces the number of independent parameters to only two: Λ and κ_W .

A fundamental property of true gauge particles is that their anomalous magnetic moments (κ_W) are equal to unity (apart from radiative corrections). Therefore, it is crucial that the particles observed at CERN meet this important criteria. On the other hand, a composite gauge boson would not be required to have $\kappa_W = 1$ unless imposed by some additional symmetry. Since we are considering the possibility of a composite boson, we leave κ_W as a free parameter. We will see that the process $\gamma e \rightarrow W\nu$ is quite sensitive to deviations in κ_W while the reactions $W \rightarrow e\nu\gamma$ and $\bar{\nu}e \rightarrow W\gamma$ are not.

In composite models of quarks, leptons, and gauge bosons there exists the possibility of new thresholds which, in principle, could compete with form-factor effects. If, however, we assume, as we do here, that the fermion com-

posite scale is much larger than that for gauge bosons then we expect form factor effects to dominate.

For further discussion of the topics considered in this paper the reader is referred to the literature.⁷

II. $W \rightarrow e\nu\gamma$

The decay rate for the process⁸ $W \rightarrow e\nu\gamma$ can be calculated from the Feynman diagrams shown in Fig. 1. The matrix element can be written in the form

$$M = \frac{ieg}{2\sqrt{2}} \bar{u}(p_1) S_{\mu\nu} v(p_2) \epsilon_\mu^\dagger \epsilon_\nu^\gamma, \quad (2)$$

where ϵ_μ^\dagger (ϵ_ν^γ) is the W -boson (photon) polarization vector and g is the electroweak coupling constant. $S_{\mu\nu}$ is given by

$$S_{\mu\nu} = (2p_1 \cdot k)^{-1} \gamma_\nu (\not{p}_1 + \not{k}) \gamma_\mu (1 - \gamma_5) + (2p_2 \cdot k)^{-1} \gamma^\sigma (1 - \gamma_5) \Gamma_{\sigma\mu\nu}^W F_P, \quad (3)$$

where

$$\Gamma_{\sigma\mu\nu}^W = \{-g_{\sigma\mu}(2p - k)_\nu + g_{\sigma\nu}[p - (1 + \kappa_W)k]_\mu + g_{\mu\nu}(p + \kappa_W k)_\sigma\} F_V$$

and F_P (F_V) is the form-factor modification of the propagator (vertex). Since the modifications F_P and F_V are of

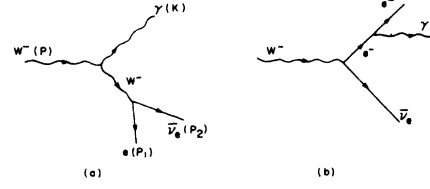


FIG. 1. Feynman diagrams for the process $W \rightarrow e\nu\gamma$.

the same form (1) we will drop the subscripts and label all corrections as F ; matrix element contributions will therefore be of three types F^2 , F^1 , or 1. We note that F^2 corrections arise from the products $F_P F_P$, $F_V F_V$, or $F_P F_V$ which are indistinguishable experimentally. For this case F is given by

$$F = \left[1 + \frac{(1-x_3)M_W^2}{\Lambda^2} \right]^{-1}.$$

Following the usual procedure we obtain the differential decay rate for this processes:

$$\frac{d^2\Gamma}{dx_1 dx_2} = \frac{\alpha^2 M_W}{512\pi x_W} G, \quad (4)$$

where

$$G = 16 \left[\frac{y_2}{y_1} + \frac{y_4}{M_W^2} \right] + \frac{2}{y_3^2} [A(2y_5 y_6 - y_4 M_W^2) + 2B y_1 y_2 + 2C(y_1 y_6 + y_2 y_5 - y_3 y_4) - 2D y_4 M_W^2] F^2 + \frac{1}{y_1 + y_3} \left[32y_4 y_5 + 16y_5 y_2 - 16y_4 y_1 - 32y_6 y_1 + 16y_3 y_4 - 16\kappa_W y_1 y_2 - \left[\frac{8y_1}{M_W^2} \right] [(1 + \kappa_W)(y_2 y_5 + y_3 y_4 + y_1 y_6) - y_4 M_W^2 - 2y_5 y_6] \right] F,$$

$$A = -1 - 2\kappa_W y_3 / M_W^2, \quad B = -2 - 2\kappa_W + \kappa_W^2, \quad (5)$$

$$C = 2 + 4\kappa_W + (1 + \kappa_W + \kappa_W^2) y_3 / M_W^2, \quad D = 4 - 4y_3 / M_W^2 - [(1 + \kappa_W) y_3 / M_W^2]^2,$$

and the y_i are given by

$$\begin{aligned} y_1 &\equiv p_1 \cdot k = \frac{1}{2}(1-x_2)M_W^2, \\ y_2 &\equiv p_2 \cdot k = \frac{1}{2}(1-x_1)M_W^2, \\ y_3 &\equiv p \cdot k = \frac{1}{2}x_3 M_W^2, \\ y_4 &\equiv p_1 \cdot p_2 = \frac{1}{2}(1-x_3)M_W^2, \\ y_5 &\equiv p_1 \cdot p = \frac{1}{2}x_1 M_W^2, \\ y_6 &\equiv p_2 \cdot p = \frac{1}{2}x_2 M_W^2. \end{aligned} \quad (6)$$

The x_i are the conventional scaling variables defined by

$$x_i = \frac{2E_i}{M_W}, \quad (7)$$

where the E_i are the energies of the final state particles in the W rest frame.

This differential decay distribution is infrared divergent upon integration over x_1 and x_2 . To eliminate this divergence we cut off the photon energy by giving the photon a small mass m_γ ($m_\gamma = \delta m_W$). In Table I the ratio $\Gamma(W \rightarrow e\nu\gamma) / \Gamma(W \rightarrow e\nu)$ is tabulated for various values of δ . We list values for SM W 's as well as for composite W 's. To obtain values for the width $\Gamma(W \rightarrow e\nu\gamma)$ we per-

TABLE I. The ratio $\Gamma(W \rightarrow e\nu\gamma)/\Gamma(W \rightarrow e\nu)$ for various values of δ . Both cases F^1 and F^2 (at $\Lambda=100,350$ GeV) are shown as well as the SM result. Two different values of κ_W are shown, $\kappa_W=+1$ and $\kappa_W=-3$.

		Λ (GeV)	$\delta=0.025$	$\delta=0.050$	$\delta=0.075$
$\kappa_W=+1$	F	100	0.019	0.011	0.008
	F	350	0.026	0.015	0.010
	F^2	100	0.014	0.009	0.006
	F^2	350	0.025	0.014	0.009
	1	∞	0.027	0.015	0.010
$\kappa_W=-3$	F	100	0.020	0.013	0.008
	F	350	0.027	0.016	0.011
	F^2	100	0.015	0.009	0.007
	F^2	350	0.026	0.016	0.011
	1	∞	0.028	0.017	0.011

form an integration of (4) over the variables x_1 and x_2 :

$$\Gamma(W \rightarrow e\nu\gamma) = \int_0^{1-\delta^2} dx_1 \int_{1-\delta^2-x_1}^{2-2\delta-x_1} dx_2 \frac{d^2\Gamma}{dx_1 dx_2}; \quad (8)$$

the results of this numerical integration can be seen in Fig. 2.

We will first examine the case where we fix κ_W to be the SM value ($\kappa_W=1$), while allowing for form-factor corrections. Form-factor corrections are of two types F^1 and F^2 . The single power corrections F^1 include modification of the gauge-boson trilinear coupling or the boson propagator but not both; the F^2 corrections allow for modification of both the vertex and propagator. We see that for F^1 , $\Lambda=100$ GeV the decay rate deviates from the SM prediction by roughly 25%. As Λ increases, deviation from the SM rapidly decreases so that for $\Lambda=250$ GeV the ratio $\Gamma/\Gamma_{\text{SM}}=0.95$, only a 5% effect. For F^2 corrections the deviation from the SM is much more pronounced. We see that for the case F^2 , $\Lambda=100$ GeV the decay rate deviates from the SM by approximately 45%; this is a much larger deviation than the case with only a single power of F . However, as Λ increases the rate at which the ratio $\Gamma/\Gamma_{\text{SM}}$ approaches unity is more rapid in

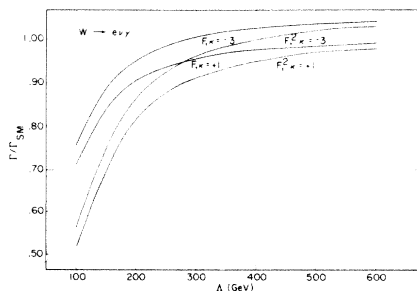


FIG. 2. The decay rate $\Gamma(W \rightarrow e\nu\gamma)/\Gamma(W \rightarrow e\nu\gamma)_{\text{SM}}$ as a function of the compositeness scale Λ ; the cases F^1 , F^2 , and $\kappa_W=1, -3$ are shown. The energy cutoff is taken to be $\delta=0.025$.

the F^2 case then the F^1 case. So, even though for small Λ the deviation from the SM is great, we cannot easily distinguish the possibility of large Λ from the SM. For example, for $\Lambda=350$ GeV we need roughly a 5% measurement to differentiate the two possibilities. Therefore, a measurement of the decay rate $\Gamma(W \rightarrow e\nu\gamma)$ provides a good test for determining the compositeness scale if Λ is less than 350 GeV. However, for Λ much greater than 350 GeV form-factor effects become almost negligible unless very precise measurements are made.

We have also examined the effect on the decay rate if we let κ_W vary. We see that the decay rate is not very sensitive to deviations in κ_W . The general shape, as well as the magnitude, of the curve remains about the same. As shown in Fig. 2 the case $\kappa_W=-3$ gives roughly a 5% deviation from the SM value. Thus, we see that this process is quite insensitive to deviations in κ_W ; therefore, it does not provide a good test for determining the magnetic moment of the W . We will see in the next section that the process $\gamma e \rightarrow W\nu$ is much more sensitive to deviations in κ_W .

III. $\gamma e \rightarrow W\nu$

Measuring the cross section for the process $\gamma e \rightarrow W\nu$ will provide an important test of the properties of the W ; this reaction should be possible at planned e^+e^- accelerators.⁹ As we will see, this reaction is not only sensitive to form-factor corrections but it is also quite sensitive to deviations in the anomalous-magnetic-moment couplings.

We evaluate the differential cross section¹⁰ for this reaction using the Feynman diagrams shown in Fig. 3. The matrix element can be written in the same form as in (2):

$$M = \frac{ieg}{2\sqrt{2}} \bar{u}(p_2) S_{\mu\nu} u(p_1) \epsilon_W^\mu \epsilon_\nu^\gamma, \quad (9)$$

where $S_{\mu\nu}$ is given by

$$S_{\mu\nu} = (2p_1 \cdot k)^{-1} \gamma_\mu (1 - \gamma_5) (\not{p}_1 + \not{k}) \gamma_\nu - (2p \cdot k)^{-1} \gamma^\sigma (1 - \gamma_5) \Gamma_{\sigma\mu\nu}^W F_P$$

and $\Gamma_{\sigma\mu\nu}^W$ is the same as in (3). The form factor F is given by

$$F = \left[1 - \frac{(M_W^2 - 2x_3)}{\Lambda^2} \right]^{-1}$$

with x_3 defined below.

Calculating the differential cross section in the usual way we obtain

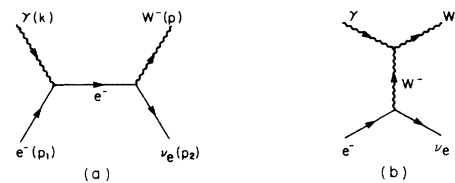


FIG. 3. Feynman diagrams for the process $\gamma e \rightarrow W\nu$.

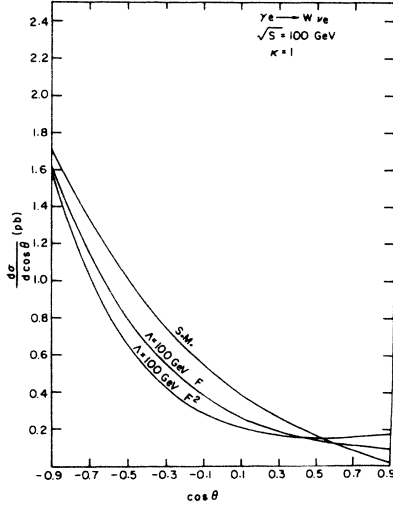


FIG. 4. The differential cross section $d\sigma/d\cos\theta(\gamma e \rightarrow W\nu)$ at $\sqrt{s}=100$ GeV and $\kappa_W=1$. Both cases F^1 and F^2 (at $\Lambda=100$ GeV) are shown as well as the SM result. The angle θ is taken to be the angle between the incoming e and the outgoing W boson in the center-of-mass frame.

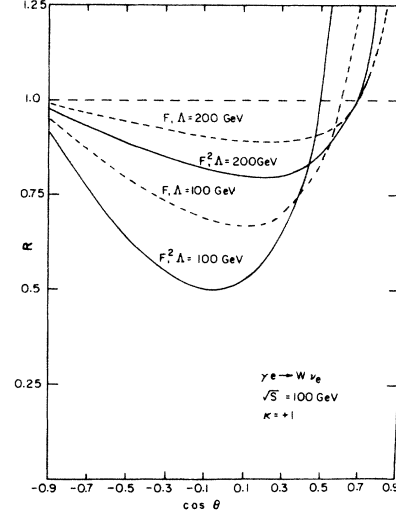


FIG. 5. The ratio R , given in Eq. (12), as a function of $\cos\theta$. Both F^1 and F^2 corrections are considered for the two scales $\Lambda=100$ GeV and $\Lambda=200$ GeV.

$$\frac{d\sigma}{d\cos\theta}(\gamma e \rightarrow W\nu) = \frac{\pi\alpha^2}{64x_W s} (1 - M_W^2/s) H,$$

$$H = 16 \left[\frac{x_2}{x_1} + \frac{x_4}{M_W^2} \right] + \frac{8}{(2x_4 + M_W^2)^2} [A(2x_5x_6 - x_4M_W^2) + 2Bx_1x_2 + 2C(x_1x_6 + x_2x_5 - x_3x_4) - 2Dx_4M_W^2] F^2$$

$$+ \frac{2}{x_1(2x_4 + M_W^2)} \left[32x_4x_5 + 16x_2x_5 - 16x_1x_4 - 32x_1x_6 + 16x_3x_4 - 16\kappa_W x_1x_2 \right. \\ \left. + \left[\frac{2x_1}{M_W^2} \right] [-2x_5x_6 + (1 + \kappa_W)(x_2x_5 + x_3x_4 + x_1x_6) - x_4M_W^2] \right] F,$$

(10)

where A , B , C , and D are given in (5) with the replacement $y_3 \rightarrow x_3$. The x_i are given by

$$x_1 \equiv p_1 \cdot k = \frac{s}{2},$$

$$x_2 \equiv p_2 \cdot k = \frac{1}{4}(s - M_W^2)(1 - \cos\theta) = -\frac{1}{2}u,$$

$$x_3 \equiv p \cdot k = \frac{1}{4}(s + M_W^2)(1 + \beta \cos\theta) = \frac{1}{2}(M^2 - t),$$

$$x_4 \equiv p_1 \cdot p_2 = \frac{1}{4}(s - M_W^2)(1 + \cos\theta) = -\frac{1}{2}t,$$

$$x_5 \equiv p_1 \cdot p = \frac{1}{4}(s + M_W^2)(1 - \beta \cos\theta) = \frac{1}{2}(M^2 - u),$$

$$x_6 \equiv p_2 \cdot p = \frac{1}{2}(s - M_W^2),$$

(11)

where $\beta = (s - M_W^2)/(s + M_W^2)$ and s , t , and u are the usual kinematic variables satisfying $s + t + u = M^2$.

The results of our calculation can be seen in Figs. 4–8. In Fig. 4 we see that allowing for form-factor effects eliminates the zero at $\cos\theta=1$. For $\cos\theta < 0.5$ the general shape of the differential cross section as a function of the $\cos\theta$ curve does not appreciably change; however, the curves with form factors are scaled down in magnitude

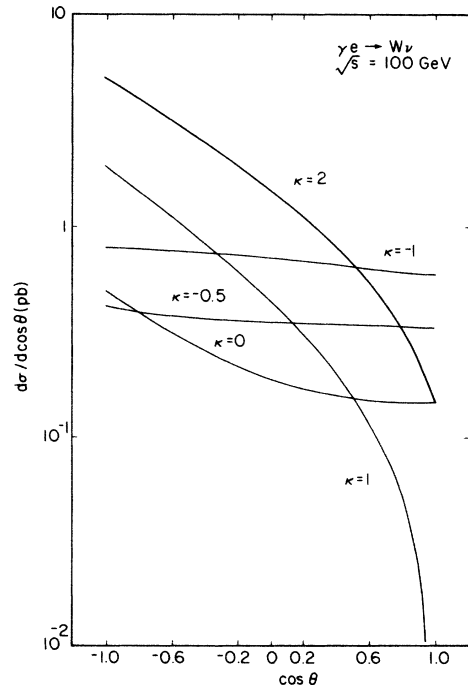


FIG. 6. $d\sigma/d\cos\theta(\gamma e \rightarrow W\nu)$ for various values of κ_W .

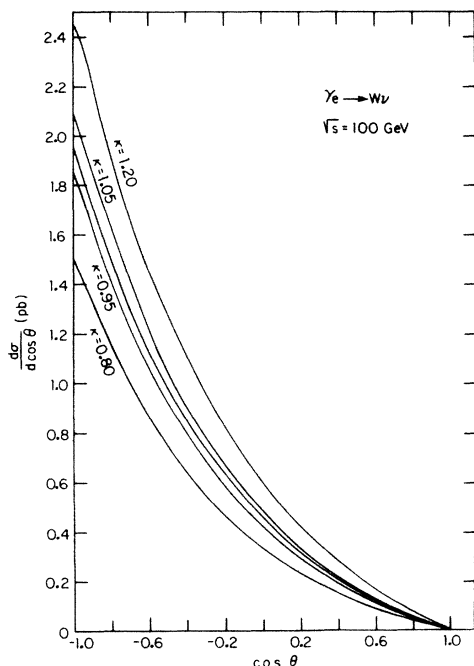


FIG. 7. $d\sigma/d \cos\theta(\gamma e \rightarrow W\nu)$ for κ_W values near unity.

from the SM prediction. The magnitude of this scaling is best illustrated in Fig. 5 where we see that for $\Lambda = 100, 200$ GeV the ratio

$$R = \frac{d\sigma/d \cos\theta}{(d\sigma/d \cos\theta)_{SM}} \quad (12)$$

significantly deviates from unity. The deviation is greatest near $\cos\theta = 0$ where for the extreme case (F^2 , $\Lambda = 100$ GeV) it is roughly 50%. In contrast with the above case we see that to distinguish the case F^1 , $\Lambda = 200$ GeV from the SM we need a 10% measurement. The curves with both corrections (F^2) are more suppressed than the F^1 case, as we would naively expect. The divergence of the graph for small angles is simply due to the

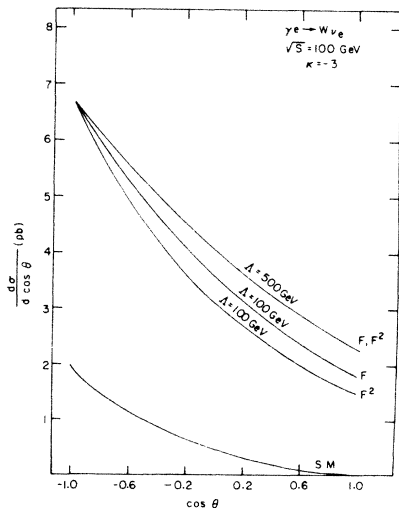


FIG. 8. The same as in Fig. 4 with $\kappa_W = -3$.

zero in the SM result. Since the total cross section for $\gamma e \rightarrow W\nu$ is approximately 1 or 2 pb (Fig. 4) we would expect ≈ 500 or so events of this kind per year at a luminosity of $10^{31} \text{ cm}^{-2} \text{ sec}^{-1}$ and so we would expect to be able to do a 10% determination of $d\sigma/d \cos\theta$ reasonably quickly.

The $\gamma e \rightarrow W\nu$ process is also very sensitive to deviations of κ_W away from unity. In Fig. 6 we see that $\kappa_W \neq 1$ not only is the magnitude of the $d\sigma/d \cos\theta$ curve significantly changed but also the *shape* of the curve. For example, at $\cos\theta = 0$ the $\kappa_W = 2$ prediction is three times as large as the SM prediction. It is also important to note that by allowing κ_W to vary eliminates the zero at $\cos\theta = 1$ allowing a clear signal for variance from the SM. In Fig. 7 we see that a measurement at the 20% level would allow us to limit κ_W to the range $0.9 < \kappa_W < 1.1$, which is a very stringent limit. In Fig. 8 we allow for the possibility of both a form-factor contribution and a nonstandard κ_W value; the situation then becomes quite confused. The effect of the form factors is to decrease the amplitude for most $\cos\theta$, while the κ_W variation depends markedly on the angle. Since the κ_W variance is largest it plays the role of the dominant factor. Thus, we have seen that the γe channel is very sensitive to both κ_W and form-factor alterations of the SM; hence, this process provides a good test for compositeness of W bosons.

IV. $\bar{\nu}e \rightarrow W\gamma$

To create a W via the process¹¹ $\bar{\nu}e \rightarrow W\gamma$ requires very-high-energy neutrinos, such neutrinos can only be found in cosmic rays; at a large neutrino detector such as DUMAND¹² such reactions should be observable.

By crossing symmetry we can obtain the diagrams for the process $\bar{\nu}e \rightarrow W\gamma$ (Fig. 9) from the diagrams of Fig. 3. The matrix element can be written in the form

$$M = \frac{ieg}{2\sqrt{2}} \bar{\nu}(p_2) S_{\mu\nu} u(p_1) \epsilon_W^\mu \epsilon_\gamma^\nu, \quad (13)$$

where $S_{\mu\nu}$ is given by

$$S_{\mu\nu} = (2p_1 \cdot k)^{-1} \gamma_\mu (1 - \gamma_5) (\not{p}_1 - \not{k}) \gamma_\nu + (2p \cdot k)^{-1} \gamma^\sigma (1 - \gamma_5) \Gamma_{\sigma\mu\nu}^W F_P,$$

where $\Gamma_{\sigma\mu\nu}^W$ is obtained from (3) by letting $k \rightarrow -k$. The form factor F is now given by

$$F = \left[1 + \frac{s}{\Lambda^2} \right]^{-1}.$$

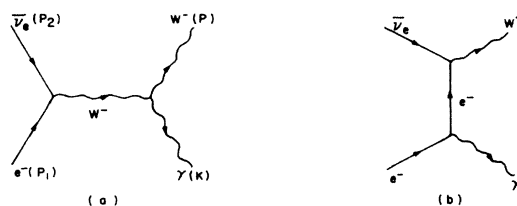


FIG. 9. Feynman diagrams for the process $\bar{\nu}e \rightarrow W\gamma$.

TABLE II. The differential cross section $d\sigma/d\cos\theta$ (pb) for the process $\bar{\nu}e \rightarrow W\gamma$. Tabulated are various values of $\cos\theta$, κ_W , and \sqrt{s} . The angle θ is defined as the angle between the incoming electron and the outgoing W boson in the center-of-mass frame.

\sqrt{s} (GeV)	κ_W	$\cos\theta$				
		-0.8	-0.4	0	0.4	0.8
100	-3	306	85.2	40.1	20.7	10.4
	1	291	74.2	31.6	13.6	3.60
	3	290	74.9	33.7	16.3	5.90
200	-3	38.7	18.8	13.8	13.2	15.9
	1	18.1	3.83	1.52	0.70	0.22
	3	20.0	6.27	4.58	4.38	4.50

The differential cross section for this process is

$$\frac{d\sigma}{d\cos\theta}(\bar{\nu}e \rightarrow W\gamma) = \frac{\pi\alpha^2}{64x_W s} (1 - M_W^2/s) H, \quad (14)$$

where H is the same as the $\gamma e \rightarrow W\nu$ case and the x_i are those in (11) with the interchange of s and t due to crossing symmetry.

In Table II we have tabulated $d\sigma/d\cos\theta$ for various cases. We see that as $\cos\theta$ approaches unity that $(d\sigma/d\cos\theta)_{\text{SM}}$ approaches zero. As in the γe case modification of the gauge couplings via either κ_W or form-factor corrections eliminates this zero. We see in Table II that this process is not very sensitive to deviations in κ_W for $\sqrt{s} = 100$ GeV. However, as \sqrt{s} increases $d\sigma/d\cos\theta$ begins to diverge from the SM (the trade off is that the magnitude of $d\sigma/d\cos\theta$ decreases substantially). In Figs. 10 and 11 we see that form-factor effects are quite substantial. For $\theta_{\text{c.m.}} > 90^\circ$ the deviation is roughly 50%. For small θ the deviation is very large (due to the SM zero

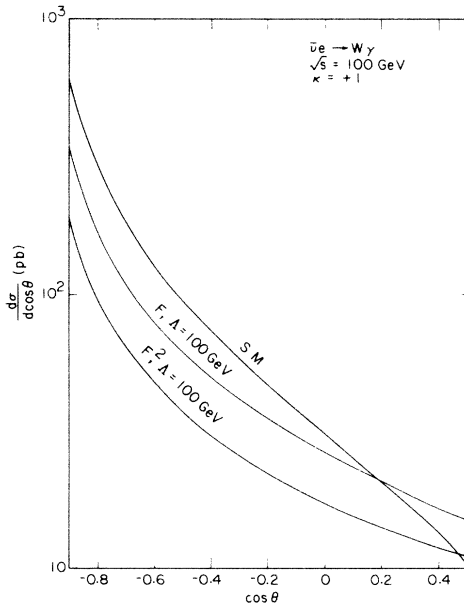


FIG. 10. The differential cross section $d\sigma/d\cos\theta(\bar{\nu}e \rightarrow W\gamma)$ at $\sqrt{s} = 100$ GeV and $\kappa_W = 1$. Both cases F^1 and F^2 (at $\Lambda = 100$ GeV) are shown as well as the SM result. The angle θ is the same as in Fig. 4.

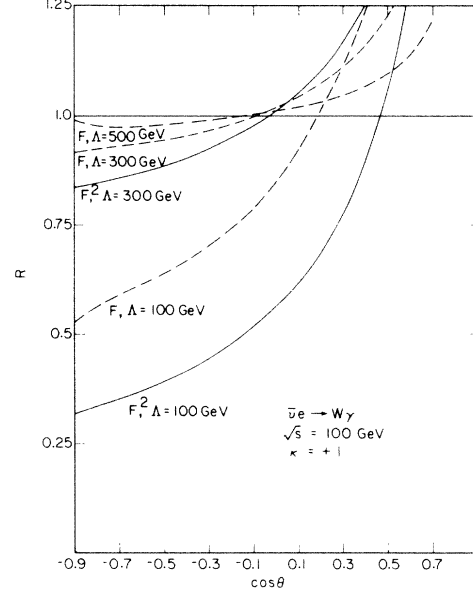


FIG. 11. $d\sigma/d\cos\theta(\bar{\nu}e \rightarrow W\gamma)$ normalized to the SM value. Both cases F^1 and F^2 are shown for various values of Λ .

at $\cos\theta = 1$) but $d\sigma/d\cos\theta$ is small. In Fig. 12 we have allowed for both a form-factor contribution and a non-standard κ_W . The result is nearly the same as in Fig. 10 with deviations being slightly greater due to the extra suppression from κ_W effects. Thus, we have seen that this process is fairly sensitive to form-factor effects but not very sensitive to κ_W effects. However, the difficulty in observing this process experimentally discounts it from being a good test for boson compositeness.

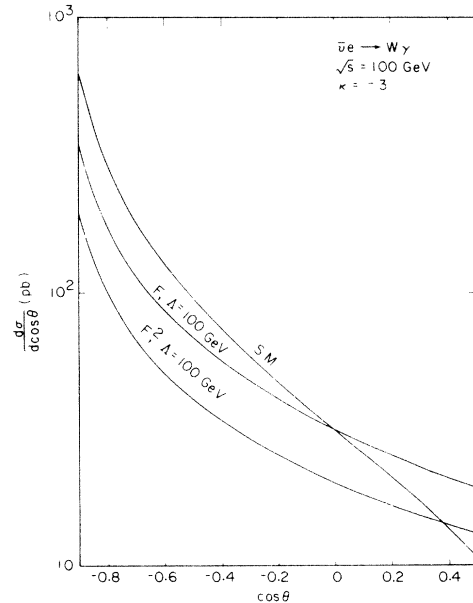


FIG. 12. The same as in Fig. 10 with $\kappa_W = -3$.

V. CONCLUSIONS

In this paper we have examined both form-factor and κ_W effects in the processes $W \rightarrow e\nu\gamma$, $\gamma e \rightarrow W\nu$, and $\bar{\nu}e \rightarrow W\gamma$. In general we have found that a composite W will have a lower decay rate/cross section than a SM W ; the deviation is greatest when both propagator and vertex corrections are taken into account. We found that all three processes give a clear signal for compositeness if $\Lambda < 350$ GeV. For $\Lambda \geq 350$ GeV it becomes quite difficult to distinguish a composite W from the SM boson, hence a study of these processes would not be very useful in constraining Λ to values much greater than 350 GeV unless very sensitive measurements were possible.

We have found that the reactions $W \rightarrow e\nu\gamma$ and $\bar{\nu}e \rightarrow W\gamma$ are quite insensitive to deviations in κ_W . On the other hand, the reaction $\gamma e \rightarrow W\nu$ is very sensitive to κ_W deviations; a precise measurement of $d\sigma/d\cos\theta$ for this reaction can constrain κ_W to values within 5% of its SM value.

In examining combined form-factor and κ_W effects we find that we have mixed results. In the $\gamma e \rightarrow W\nu$ case the κ_W effect is dominant while in the other two cases form-factor effects are most pronounced.

It is quite possible that future experiments will uncover another substructure of matter. We have found that the $WW\gamma$ vertex is very sensitive to form-factor and κ_W effects; hence, processes containing this vertex will provide an early signal for physics beyond the SM.

¹UA1 Collaboration, G. Arnison *et al.*, Phys. Lett. **122B**, 103 (1983); **126B**, 398 (1983); UA2 Collaboration, G. Banner *et al.*, *ibid.* **122B**, 476 (1983); P. Bagnaia *et al.*, *ibid.* **129B**, 130 (1983).

²S. Weinberg, Phys. Rev. Lett. **19**, 1264 (1967); Phys. Rev. D **5**, 1412 (1972); A. Salam, in *Elementary Particle Theory: Relativistic Groups and Analyticity (Nobel Symposium No. 8)*, edited by N. Svartholm (Almqvist and Wiksell, Stockholm, 1968), p. 367; S. Glashow, J. Iliopoulos, and L. Maiani, Phys. Rev. D **2**, 1285 (1970).

³T. G. Rizzo, Phys. Rev. D **32**, 43 (1985).

⁴See Ref. 3 and the references therein.

⁵See, for example, E. Eichten, I. Hinchliffe, K. Lane, and C. Quigg, Rev. Mod. Phys. **56**, 579 (1984).

⁶H. Aronson, Phys. Rev. **186**, 1434 (1969); K. J. Kim and Y.-S. Tsai, Phys. Rev. D **7**, 3710 (1973).

⁷See, for example, Ref. 6; J. A. Robinson and T. G. Rizzo, Ames Laboratory Report No. IS-J-1332(rev.), 1984 (unpublished); M. Suzuki, Phys. Lett. **153B**, 289 (1985); M. A. Samuel, Phys. Rev. D **31**, 1748 (1985); J. Reid, M. A. Samuel, and M. Laursen, *ibid.* **30**, 1588 (1984); F. Herzog, Phys. Lett. **148B**, 355 (1984).

⁸A. Grau and J. A. Grifols, Phys. Lett. **148B**, 358 (1984); T. R. Grose and K. O. Mikaelian, Phys. Rev. D **23**, 123 (1981).

⁹See, for example, F. M. Renard, Z. Phys. C **14**, 209 (1982), and references therein.

¹⁰K. O. Mikaelian, Phys. Rev. D **17**, 750 (1978); **30**, 1115 (1984); A. Grau and J. A. Grifols, Nucl. Phys. **B233**, 375 (1984).

¹¹R. W. Brown *et al.*, Phys. Rev. D **20**, 1164 (1979).

¹²See, for example, *Proceedings of the 1980 DUMAND Symposium Honolulu*, edited by V. J. Stenger (Hawaii DUMAND Center, Honolulu, 1981).